J Membrane Biol (2010) 235:1–15
DOI 10.1007/s00232-010-9249-2

ORIGINAL ARTICLES

Examining the Origins of the Hydration Force Between Lipid Bilayers Using All-Atom Simulations

Anastasia N. Gentilcore · Naveen Michaud-Agrawal · Paul S. Crozier · Mark J. Stevens · Thomas B. Woolf

Received: 11 March 2010 / Accepted: 11 March 2010 / Published online: 13 April 2010

Abstract Using 237 all-atom double bilayer simulations, we examined the thermodynamic and structural changes that occur as a phosphatidylcholine lipid bilayer stack is dehydrated. The simulated system represents a micropatch of lipid multilayer systems that are studied experimentally using surface force apparatus, atomic force microscopy and osmotic pressure studies. In these experiments, the hydration level of the system is varied, changing the separation between the bilayers, in order to understand the forces that the bilayers feel as they are brought together. These studies have found a curious, strongly repulsive force when the bilayers are very close to each other, which has been termed the "hydration force," though the origins of this force are not clearly understood. We computationally reproduce this repulsive, relatively free energy change as bilayers come together and make qualitative conclusions as to the enthalpic and entropic origins of the free energy change. This analysis is supported by data showing structural changes in the waters, lipids and salts that have also been seen in experimental work. Increases in solvent ordering as the bilayers are dehydrated are found to be essential in causing the repulsion as the bilayers come together.

Keywords Hydration force · Molecular dynamics · Entropy:enthalpy compensation · Multilayer lipid system

All authors contributed equally to this work.

A. N. Gentilcore · N. Michaud-Agrawal · T. B. Woolf (✉)
Department of Physiology, Johns Hopkins University, School of Medicine, Baltimore, MD, USA
e-mail: twoolf@jhmi.edu

P. S. Crozier · M. J. Stevens
Sandia National Laboratories, Albuquerque, NM, USA

Introduction

Though the interactions of lipid bilayers are fundamental to much of biology and medicine, there are still many aspects about the specific nature of these interactions that remain mysterious. The question of how bilayers interact within a multilayer stack has been studied experimentally using the surface force apparatus (Marra and Israelachvili 1985), atomic force microscopy (Pera et al. 2004; Abdulreda and Moy 2007) and osmotic stress (LeNeveu et al. 1977; Parsegian et al. 1979; Rand and Parsegian 1989) over many years. In addition, an extensive body of continuum theory (Petrache et al. 1998; Israelachvili 1985; Derjaguin and Landau 1941; Verwey and Overbeek 1948; Helfrich 1978; Podgornik and Parsegian 1992; Sornette and Ostrowsky 1986; Leikin et al. 1993; Marcelja and Radic 1976; Israelachvili and Wennerstroem 1990, 1992, 1996) exists to rationalize these interactions. However, explaining the origins of repulsive forces at low hydration, termed "hydration forces," remains a hotly debated topic. Answering these questions about forces between bilayers is essential for understanding biological processes like endocytosis and membrane fusion. Armed with a molecular understanding of these events, great strides could be made in rational bioengineering efforts, e.g., in controlling drug delivery by accurately predicting the properties and interactions of the lipid vesicle encasements to allow the introduction of drugs directly into cells.

Continuum Theory

Experiments have shown that, for many lipid types, when water is added to unoriented multilamellar lipid vesicles, the stack will swell until the interbilayer distance reaches some value, D_0, after which any additional water separates

into another phase containing monomeric lipids (Petrache et al. 1998). Thus, there exists a long-range attractive van der Waals force between bilayers, which accounts for the finite swelling behavior. Since the stack remains multilamellar and does not condense into one homogeneous phase, there must also be a repulsive force keeping the bilayers apart from each other (Petrache et al. 1998).

Initial attempts to describe the interactions between two surfaces in an aqueous solution explained the phenomenon as a balance between electrostatic repulsive double-layer forces and van der Waals attractive forces (Israelachvili 1985). The van der Waals force between two bilayers has the form (Manciu and Ruckenstein 2001)

$$V_{\mathrm{vdw}}(z) = -\frac{H}{12\pi}\left(\frac{1}{(z+t_{\mathrm{h}})^2} + \frac{1}{(z+t_{\mathrm{h}}+2t_{\mathrm{c}})^2} - \frac{2}{(z+t_{\mathrm{h}}+t_{\mathrm{c}})^2}\right) \tag{1}$$

where H is the Hamaker constant, t_{h} is the thickness of the lipid head groups, t_{c} is the thickness of the lipid chains and z is the distance between two bilayers. However, this theory is not sufficient to explain the more complex behavior of bilayer surfaces interacting because, unlike the assumed smooth surfaces of the theory, bilayers have large-scale undulations, small-scale protrusions and complex microscopic lipid head group, water and salt interactions that are not accounted for in the theory.

Therefore, an additional theory was developed to consider the flexible nature of these assemblies. A bilayer isolated in solution will have a large number of undulatory and compressive modes that may be explored. However, when this bilayer is close to other bilayers, many of these modes will not be sterically accessible due to the proximity of the other bilayers. This reduction in conformations available to the systems results in a decrease in entropy and therefore a repulsive force between the bilayers as they move closer to each other. Helfrich (1978) proposed a repulsive term of the form

$$f_{\mathrm{c}} = \frac{(kT)^2}{128K_{\mathrm{c}}\sigma_{\mathrm{b}}^2} \tag{2}$$

where k is Boltzmann's constant, T is the temperature, K_{c} is the bilayer bending modulus and σ_{b}^2 is the mean square fluctuation of the bilayer.

However, other groups (Podgornik and Parsegian 1992; Sornette and Ostrowsky 1986) have suggested an alternative form for this force, arguing that the confinement of the bilayers is not as strong as proposed by Helfrich (1978). The confinement is not purely steric because each bilayer can adjust to the confinement enforced by its neighbors and mitigate the effects of this confinement. This less extreme confinement has been termed "soft" confinement and has the form

$$f_{\mathrm{sc}} = \frac{\pi kT}{16}\left(\frac{A_{\mathrm{H}}}{K_{\mathrm{c}}\lambda^2}\right)^{1/2} e^{-a/2\lambda} \tag{3}$$

where A_{H} is the hydration force fit constant, λ is the exponential decay length and a is the average bilayer separation distance.

What has most puzzled researchers studying the interactions of bilayers is the behavior when the bilayers are quite close together, with less than 15 Å of water thickness between them. In this regime, strong repulsive forces with an exponential character have been measured that cannot be accounted for using any of the previously mentioned theories (Leikin et al. 1993). These forces between two neighboring planar bilayers have the form

$$V_{\mathrm{H}}(z) = A_{\mathrm{H}}e^{-z/\lambda} \tag{4}$$

and have been termed "hydration forces" because it is thought that the interactions between the surface and the solvent cause them, though the exact mechanism is unclear (Leikin et al. 1993). In one major proposed explanation, the energetic penalty incurred to desolvate the surfaces so that the two surfaces may come directly into contact outweighs any attraction the surfaces may have. In other words, it is difficult (energetically unfavorable) to remove the final waters which hydrate the bilayers to bring the surfaces together. Though there is theory to support this work (Marcelja and Radic 1976) and while it has been possible to come to some agreement as to the exponential character of this force by fits to experimental data, there is still much debate as to the origins of the force. Other theorists (Israelachvili and Wennerstroem 1990) propose that this force is due to lipid head group protrusions. In this theory, electrostatic interactions between the positively and negatively charged parts of the lipid head groups cause the head groups to protrude into the gap between the bilayers and create steric repulsion forces.

For greater insight into the nature of the forces between bilayers, we set up a bilayer stack mimetic system and varied the hydration level. We estimated the relative free energy change as the bilayers come together, a quantity directly related to the force, which indicates whether the interaction is attractive or repulsive in character. We also examined how entropic/enthalpic compensation underlies this estimate. Further detailed analysis of the microscopic changes in the waters, lipids and salts helps support these results.

Methods

To further understand bilayer-to-bilayer interactions, we have made a stacked lipid bilayer mimetic system where the hydration level can be explicitly controlled. Figure 1

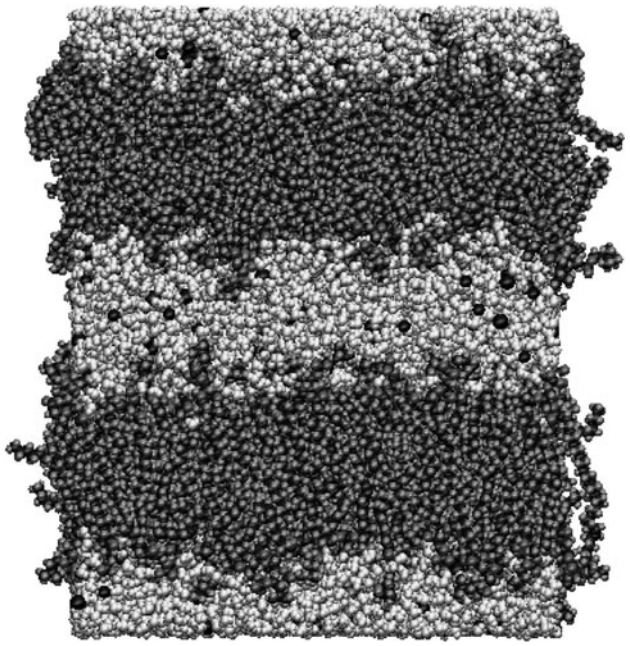

Fig. 1 Representative all-atom double bilayer system used in this study. *Dark sections* are the POPC lipids, while *lighter sections* represent the solvent. Image created using VMD (Humphrey et al. 1996)

shows a representative double bilayer system used in this study. The size and number of components for the initial double bilayer systems were chosen to be consistent with the work of Sachs et al. (2004a) so that this work could be compared to that analysis. The initial set-up began with an equilibrated 1-palmitoyl-2-oleoylphosphatidylcholine (POPC) lipid bilayer system from the Feller group, which was expanded to be a double bilayer system of 512 total lipids by replicating the system in all dimensions. Waters and salts were added to bring the total to 6,144 TIP3P (Jorgensen et al. 1983) waters per bath and 120 sodium and chloride ions per bath. The system measured approximately 90 Å in the x and y directions and 120 Å in the z dimension (the direction normal to the bilayer).

The x and y dimensions were held fixed in all simulations instead of assuming constant pressure in the x and y directions. The rationale is that though a biological vesicle or other membrane assembly has well-defined surface tension in response to the standard 1 atm of pressure it feels, a micropatch does not have all of the same undulatory modes accessible to it. Thus, 1 atm of pressure exerted on the patch will cause it to respond in nonphysical ways. In a coarse-grained system with almost identical system size and makeup but no harmonic spring restraint (N. Michaud-Agrawal, personal communication), surface tension was seen to increase as the bilayers come together, which suggests the same increase would occur in our atomistic systems.

In the initial system the bilayers are farthest apart, and for each subsequent system the bilayers are positioned closer together. To accomplish this closer spacing of the bilayers while keeping the concentration constant, one sodium ion, one chloride ion and 51.2 waters (number of actual waters removed was rounded to the nearest whole) were removed from each bath. The waters were removed by slicing out the middle of the center bath and slicing off the two ends of the cell. The two halves of the system were then pushed together and the cell was resized in z. The systems were equilibrated with constant x and y dimensions and 1 atm of constant pressure in the z direction for approximately 0.7 ns to let the cell z-dimension length assume the equilibrium value characteristic of this new system.

Systems were built in groups of eight using the last of the previous group of eight systems as a starting point. This process ensured that each new group was built from a similar system and allowed for a relatively short equilibration time. Originally, the final cell z-dimension length of the equilibrium simulation was used as the initial cell z-dimension length for the production runs. However, in order to get better coverage of the bilayer separation distance reaction coordinate, for the last approximately two-thirds of the simulations built, the cell z-dimension length for each group of eight systems built was set by linearly spacing the cell z-dimension lengths between the largest and smallest lengths at the end of the equilibration runs.

As outlined above, systems were built for each integer number of ions, starting with 120 ions per bath and shrinking to four ions per bath. However, these 116 systems were not enough to completely sample the full bilayer separation distance reaction coordinate. Though the initial systems were spread out linearly to cover the intervening bilayer separation distance reaction coordinate, because of finite sampling capabilities, the mean of the histograms of bilayer separation distance values deviated from the ideal mean for the system. Thus, there were gaps between each sequential system which had to be filled with other systems to sample the space fully and ensure a meaningful free energy estimate. To achieve improved sampling, we took the systems abutting the gaps and modified their cell z-dimension length to sample the gap region. This process was not perfect as there was no way to predict what space the new systems would actually sample. Ideally, with much longer simulation times, the initial 116 systems would have sampled more evenly and this extra step may have been avoided. Figure 2 highlights the uniformity of sampling achieved across the bilayer separation distance reaction coordinate using this large number of systems. We sampled from about 22.8 Å of water between the bilayers to about 3.8 Å. Of course, the amount of sampling yielded a large data set, in excess of 2.5 terabytes (see below for sampling rates).

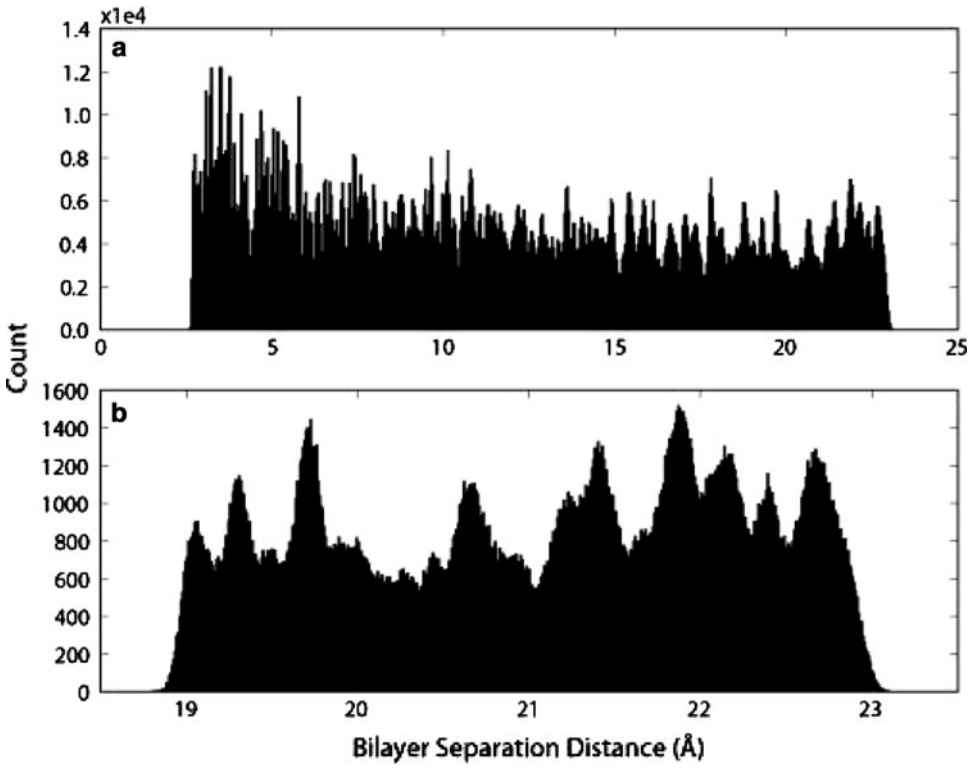

Fig. 2 Histograms of all data points sampled along bilayer spacing reaction coordinates demonstrating thoroughness of sampling for **a** all data sets and **b** a sample of one section of the reaction coordinate

In order to calculate the relative free energy change using umbrella sampling, a harmonic spring potential was set between all atoms of the two bilayers, with a spring strength of 2 kcal/Å^2 mol. The length of the spring was determined by the cell z-dimension length set after equilibration; it was half of the cell z-dimension length value. The production runs were all with constant NVT so as not to add another force/energy term to be corrected for in the free energy calculations, and the temperature was set at 298 K. The simulations used a 10 Å real-space cutoff and employed full particle–particle particle–mesh (PPPM) electrostatics (Hockney and Eastwood 1989). Initial system setup and equilibration were performed in-house using CHARMM (Brooks et al. 1983), but full equilibration and 10 ns production runs were completed on Sandia National Labs supercomputers using the Large-scale Atomic/Molecular Massively Parallel Simulator (LAMMPS, http://lammps.sandia.gov) (Plimpton 1995) with the CHARMM all-atom potential energy function and lipid parameter set PARAM 27 (Feller et al. 2002; Feller and MacKerell 2000; Schlenkrich et al. 1996). Equilibration time was about 0.7 ns for most systems, but for the closest systems this was doubled to 1.4 ns. The time step was 2 fs as the SHAKE algorithm (Ryckaert et al. 1977) was employed to fix the bond length of bonds to hydrogens. Coordinates were stored every 1 ps for a total of 10,000 frames per simulation, though some of the gap-filling systems were stored every 10 ps to save space. With the exception of the hydrogen bonding analysis, which was calculated using CHARMM, all analyses were performed using the MDAnalysis toolkit (http://code.google.com/p/mdanalysis/).

As electrostatic interactions were presumed to be a significant contributor to the interactions between bilayers as they approach one another, a double bilayer system (Sachs et al. 2004a) was employed to allow transient potential differences to develop across the bilayer, even though there were periodic boundary conditions in all dimensions. In a single, periodically connected bilayer system it would be impossible to have a potential difference across the bilayer because the bath on one side of the bilayer is periodically connected to the bath on the other side of the bilayers; they are, in essence, the same bath.

Though there is ongoing debate, a recent value for the area per lipid for POPC from the Nagle group is 68.3 ± 1.5 Å^2 for a fully hydrated system (Kučerka et al. 2006). The Nagle group also measured a phosphate-to-phosphate thickness of 37.6 Å and 31.0 waters per lipid at full hydration (Kučerka et al. 2006). Our initial system with the bilayers far apart has 24 waters per lipid, and we progress to 0.8 waters per lipid (the free energy calculation ends at 2 waters per lipid). Dehydration has been shown experimentally to reduce the area per lipid and in turn increase the bilayer thickness. Since our systems assume constant surface area throughout, we chose an area per lipid of 64.0 Å, which represents a slightly less than fully hydrated, thicker bilayer. The initial systems have a

phosphate-to-phosphate thickness of about 38.4 Å, but this value drops dramatically by about 1.8 Å as the bilayers get close to each other (data not shown). It is a matter of debate as to what measurement constitutes the true bilayer thickness, but for this work the bilayer thickness was computed by calculating the average phosphate position for each bilayer over the length of the simulation and assuming the bilayer thickness was the region between the two average phosphate positions. When the bilayers are at small separations, this metric is bound to be less well-defined since there are fewer water molecules available to form distinct water layers.

Our simulation conditions and experimental measurement systems differ in the way that they control pressure. Experimental measurements frequently vary the pressure as a way to understand the forces between bilayers. For example, surface force apparatus (Marra and Israelachvili 1985) and atomic force microscopy (Pera et al. 2004; Abdulreda and Moy 2007) physically push the bilayer stack together to vary the pressure. This process modifies the amount of available volume and water between the stacks as the bilayers are forced closer together. In our simulation conditions we are not readily able to replicate the experimental conditions due to the large system sizes that would be required to set up a true multilayer stack and the long sampling times needed to force the bilayers together with pressure as the control variable. A particular problem with simulating the experimental conditions is that, ideally, the amount of water between the stacks is controlled via a grand canonical setting, where for a given separation between the bilayers the amount of water is optimally adjusted during the simulation to sample on all possible amounts of water.

To simplify our calculations, we make two assumptions. First, we assume that the forces between the bilayers can be measured in the absence of an applied normal pressure; the force is due to the nature of the interactions between the two bilayers. Second, we assume that the distribution of waters between the two bilayers is dominated by the available volume between the two surfaces and that we can estimate that optimal number from a consideration of volume alone. In classical statistical mechanics, it is often the case that averages computed by considering the optimum of the distribution are nearly identical to those computed using the full distribution. This is because the optimum is frequently not just a bit more likely but dramatically more likely to visit in conformation space. There is of course a possible systematic error due to the fluctuations in the particle numbers between the surfaces as a function of bilayer-to-bilayer distance, which we have no easy way to measure; but the size of the error has to do with the fluctuations in the amount of matter between the surfaces at each separation and should be small relative to the error associated with sampling on the conformations at a given separation. One can think of the approach as generating an estimated relative free energy surface that is bounded on each side by the surfaces including particle number fluctuations. Making these assumptions creates a simulation ensemble that differs from the experimental ensemble. In principle, it should be possible to understand how to convert from one ensemble to the other, similar to transformations of thermodynamic quantities from one ensemble to another. In practice, a direct conversion is difficult and analysis of the systems as simulated gives the most direct connections to the molecular interactions between the two bilayers as a function of the normal distance.

The relative free energy change was calculated using free energy perturbation (FEP) (Zwanzig 1954). Our perturbations consisted of linear expansions and contractions of the systems in the z dimension (both directions were included for double-wide sampling). We made these small perturbations to 1,000 frames (every 10 ps) of each of our runs and averaged these to estimate the relative free energy changes. The continuum model curves for free energy used the following values for their parameters. For the van der Waals force (Eq. 1), we used 27.1 Å for the hydrocarbon thickness and 9.0 Å for the head group thickness (Kučerka et al. 2006); and though the Hamaker constant has been shown to depend on bilayer spacing (Podgornik et al. 2006), 4.3×10^{-21} J is a reasonable value for small spacing. The Helfrich contribution (Eq. 2) was modeled using $\sigma^2 = \mu a^2$ (Helfrich 1978), assuming uncorrelated adjacent bilayers, so $\sigma^2 = 2\sigma_b^2$, and with a μ of 0.183 (Podgornik and Parsegian 1992), where sigma is the mean square fluctuation in the water spacing and μ is a constant. The bilayer bending modulus, K_c, for POPC was set at 8.5×10^{-20} J, a value that was measured by the Nagle group (Kučerka et al. 2006) and found not to vary with bilayer spacing. For the soft confinement and hydration force terms (Eqs. 3, 4), we set A_H to 0.035 J/m^2 and λ to 2.1 Å as estimated by fits to experimental data (Manciu and Ruckenstein 2001), though the range of possible values for these constants is rather large. Enthalpic interaction energies were calculated using a modified version of LAMMPS. Diffusion constants were calculated from the slope of the mean square displacement, using the last three-fourths of each nanosecond for the fit.

Entropy Calculations

To calculate the change in entropy due to changes in the water layers for the different systems, we used an entropy estimation method developed by the Lazaridis (1998) group, which examines how a solute affects the water order surrounding it. Theoretically, the effect on the solvent–

solvent entropy of adding a solute to a box of solvent will be so small as to be indistinguishable from the situation with pure solvent because most of the solvent will be unperturbed. Therefore, to isolate this small effect, this theory places the solute at the point of origin and examines the effect of the solute field on the surrounding solvent density.

The theory relies on separating entropy contributions out by spatial and orientational correlation functions and using these functions to estimate entropy. The solvent-to-solute correlation entropy is

$$S_{\mathrm{sw}} = -k\rho_{\mathrm{w}}^{\mathrm{o}} \int [G_{\mathrm{sw}} \ln G_{\mathrm{sw}} - G_{\mathrm{sw}} + 1]\mathbf{dr} \tag{5}$$

The solvent reorganizational entropy from correlations is

$$\Delta S_{\mathrm{ww}}^{\mathrm{corr}} = -\frac{1}{2}k\rho_{\mathrm{w}}^{\mathrm{o}2} \int G_{\mathrm{sw}}(\mathbf{r}) \left[G_{\mathrm{sw}}(\mathbf{r}\prime) \left\{ g_{\mathrm{ww}}^{\mathrm{inh}} \ln g_{\mathrm{ww}}^{\mathrm{inh}} - g_{\mathrm{ww}}^{\mathrm{inh}} + 1 \right\} - \left\{ g_{\mathrm{ww}}^{\mathrm{o}} \ln g_{\mathrm{ww}}^{\mathrm{o}} - g_{\mathrm{ww}}^{\mathrm{o}} + 1 \right\} \right] \mathbf{drdr}' \tag{6}$$

where $\rho_{\mathrm{w}}^{\mathrm{o}}$ is the pure solvent density, G_{SW} is the solute–solvent correlation function with respect to the conditional solvent density at large distances from the solute, $g_{\mathrm{ww}}^{\mathrm{o}}$ is the solvent-to-solvent correlation function, $g_{\mathrm{ww}}^{\mathrm{inh}}$ is the inhomogeneous solvent-to-solvent correlation function and $\mathbf{r}$ and $\mathbf{r}'$ are the particle positions with respect to the central particle. However, since our systems are periodic in z, orientational effects are ignored and z position is the quantity of interest.

Ideally, one would calculate one-body interactions, two-body interactions, three-body interactions and so forth. However, the Kirkwood superposition approximation expresses the triplet correlation function in terms of pair correlation functions and allows all terms above the two-body term to be ignored. The formalism was developed in the canonical ensemble to allow ease of calculation of partial molar properties. It was also developed assuming constant pressure so that when the solvent is put in the box, the box size will expand to accommodate it.

The method estimates the inhomogeneous partial molar entropy, which is the entropy of solution with the entropy of pure solvent interactions subtracted out. A flat bulk density distribution has zero entropy, while distributions with order contribute unfavorably to excess entropy. In our use of this method, we subtract out the entropy of the initial system with the largest separation instead of the pure solvent because we are more interested in the relative entropy change as the bilayers come together.

This theory estimates the solvent entropy relative to a fixed solute, and in our case the solute is the entire bilayer and the solvent is just the water molecules. Bilayer fluctuations in separation as a whole are on the order of 0.05 Å, so the bilayers are relatively fixed. Since our system is symmetric in the z direction, our calculations have been performed using the z coordinate instead of $\mathbf{r}$ from a central origin. We chose the nitrogen atoms of the lipid head groups to represent the solute positions, so the two-body term is the water-to-water correlation function relative to the positions of each nitrogen atom. The calculation was repeated 10 times using each nanosecond of data as an independent data set so that error bars could be assessed. The reported error bars are the standard deviation seen from the mean of the set of 10. The two-body calculations are computationally intensive, scaling as n^2, so we used a relatively coarse grid (20 bins) for our density functions, thus introducing some systematic error into our calculations.

Results and Discussion

Our calculated free energy curve in Fig. 3 shows a strong repulsive contribution to the free energy as the bilayers approach. We also plot two different continuum model predictions, one using Helfrich undulation repulsive forces as described in Eq. 2 and one using "soft confinement" forces described by Eq. 3. Both model curves include the van der Waals interaction described in Eq. 1 and the hydration force described in Eq. 4. The free energy change we see is a few times as large as that predicted by the models but similar in overall shape. The increased magnitude of the repulsive force in comparison with experiment is most likely due to the fact that the lipids in our simulations have a set area per lipid, so the bilayers are not able to thicken in response to dehydration as they would experimentally. The calculated free energy curve also is more repulsive at larger bilayer separation distances in comparison with the theoretical curve, where there is essentially no repulsive force for large separation distances. However, comparing the separation distances directly is difficult because the theoretical work uses simplified bilayers where separation distance is well-defined but the theory rests upon experimental work, where defining bilayers separation distance is much more difficult. The Nagle group (Petrache et al. 1998) analyzed X-ray diffraction data to determine the contributions from undulation, van der Waals and the experimentally defined hydration forces to the total measured force between bilayers. They found that the undulation repulsion dominates at water layer thicknesses greater than 13 Å. A repulsion that depends exponentially on the separation is observed in these experiments when the separation distances are 5–13 Å and is called "hydration force by convention." Since our bilayer patch is small, undulation forces likely do not come into play. Thus, the repulsive force we are seeing is the result of the interactions between water and lipids that is termed the "hydration force."

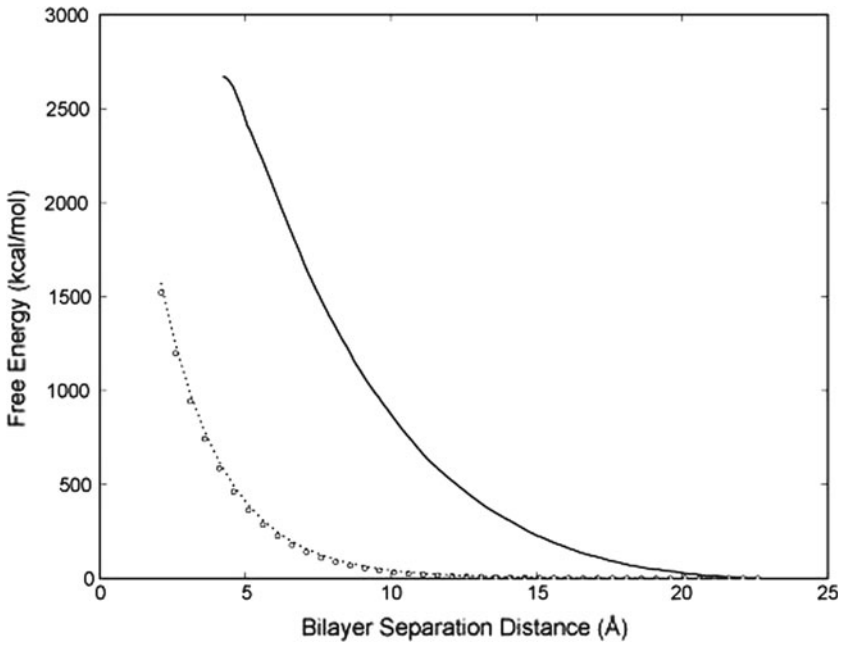

Fig. 3 Relative free energy change as a function of bilayer spacing shows an overall repulsive character to the interaction. Bilayer separation distance is shown in terms of water layer thickness for all figures. Our calculation is for relative free energy (*solid*) compared to continuum theory models consisting of van der Waals forces from Eq. 1, hydration forces from Eq. 4 and Helfrich undulation forces from Eq. 2 (*circles*) or "soft confinement" forces from Eq. 3 (*dotted*)

Possible sources of error in this calculation include the use of a fixed surface area throughout the series of simulations since experimentally the area per lipid decreases with dehydration. This choice was made because there is no clear way to model the change in area per lipid as we changed the lipid hydration. As a result, our bilayers likely experienced increasing surface tension as the bilayer-to-bilayer distance decreased, as seen in an analogous coarse-grained study (N. Michaud-Agrawal, personal communication). In experimental systems, the bilayer thickness will increase as hydration is decreased; but ours is fairly constant, then decreases by 1.8 Å as the bilayers come close to each other (data not shown). Insufficient sampling could also be a source of error. Ideally, multiple runs of the systems would be done from various starting configurations, to ensure a more comprehensive sampling of phase space. The use of a harmonic constraint between the two bilayers introduces systematic error into the calculations. The bilayer fluctuations in separation are on the order of 0.05 Å, while in experimental systems on much larger bilayer patches they are significantly larger, on the order of 2–5 Å (Petrache et el. 1998). Also, while a high salt concentration was used to ensure sufficient salt sampling, when the bilayers are quite dehydrated, the number of salt ions becomes very few, so sampling is much less reliable.

Since free energy is made up of both entropic and enthalpic energies, we sought to estimate both quantities to determine how each contributes to the total free energy. Experimental work from the Heerklotz lab (Binder et al. 1999) measures the free energy, enthalpy and entropy of dehydration of POPC using humidity titration calorimetry. They find significant contributions from each at hydration values less than about 5 waters per lipid. Their measurements for free energy show a repulsive free energy of about 2 kcal/mol at about 2 waters per lipid. They find the entropic contribution increases from essentially zero for high hydration to about 6 kcal/mol at about 2 waters per lipid. They find an enthalpic contribution with a similar curve, though of the opposite sign. Another group (Markova et al. 2000) has measured similar results using double-twin calorimetry.

In our water entropy calculations (Fig. 4), we see about a 5-kcal/mol change in entropy going from about 24 waters per lipid to 2 waters per lipid. The entropy calculations were made using the Lazaridis (1998) entropy method, which determines the bilayer's effect on the water order around it. It examines how water is ordered relative to the bilayer (Fig. 4b) and relative to both other waters and the neighboring bilayer (Fig. 4c). This method only considers the water contribution to entropy and does not explore possible contributions from the lipid bilayers themselves. The decreases in entropy as the bilayers come closer together mean that as the bilayers come into contact, increased order can be seen in the water layer. This increase in water order is also borne out by examination of water diffusion rates (Fig. 5a, b), which are greatly slowed as the bilayers move toward each other. The water diffusion rates decrease from 1.0×10^{-6} to 2.9×10^{-9} cm^2/s laterally and from 1.4×10^{-7} to 2.0×10^{-9} cm^2/s in the z direction. At 25°C, the bulk water diffusion rate is about 2.3×10^{-5} cm^2/s (Mills 1973). However, directly comparing our calculated two-dimensional lateral diffusion and

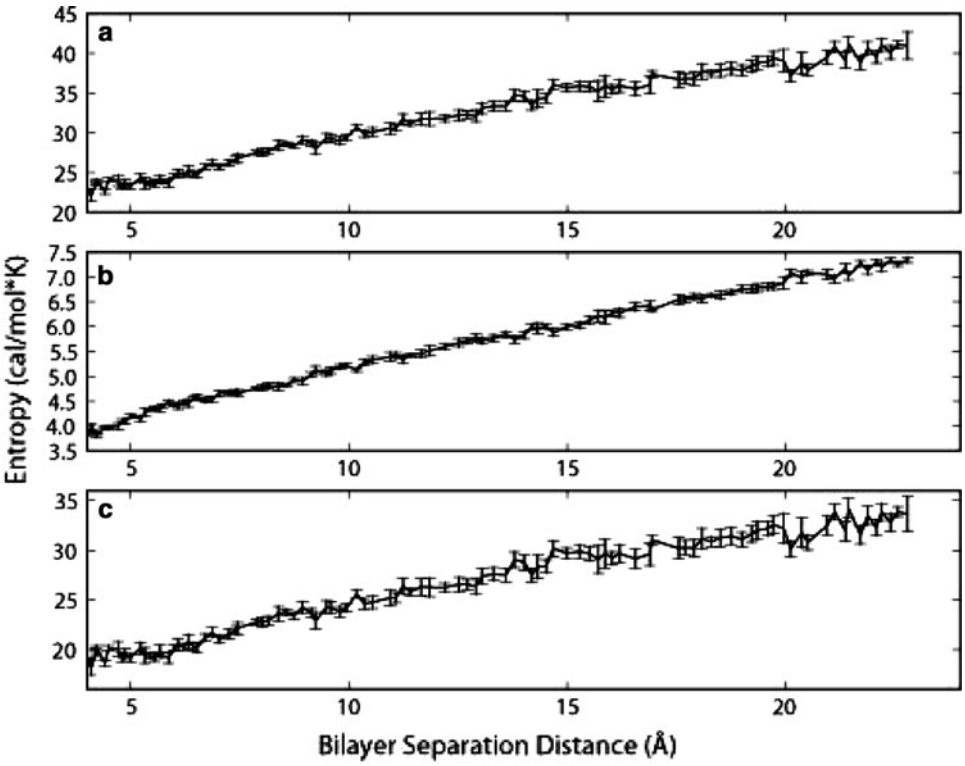

Fig. 4 Lazaridis entropy calculations show reduction in entropy as bilayer separation becomes smaller: **a** the total entropy, **b** the bilayer-to-water correlation entropy and **c** the solvent reorganizational entropy from correlations

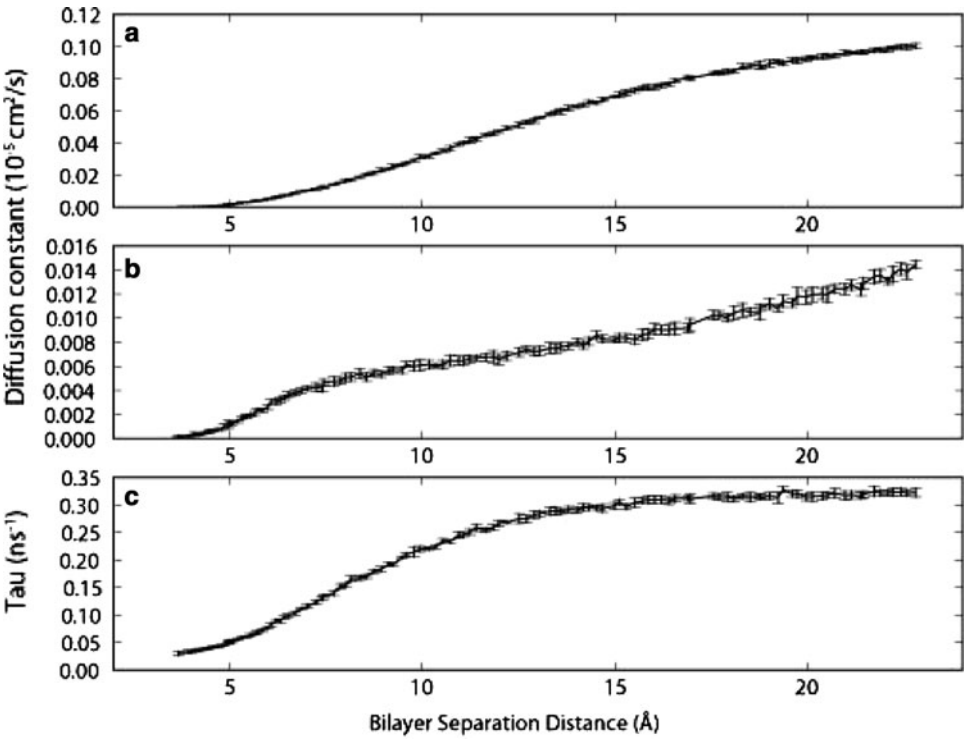

Fig. 5 Water diffusion rates and rotational autocorrelation coefficient decrease with loss of hydration: **a** lateral diffusion, **b** diffusion in the *z* direction and **c** the coefficient of rotational autocorrelation between dipole moments

one-dimensional *z*-direction diffusion rates to a bulk three-dimensional diffusion rate is not possible. The water dipole rotational autocorrelation coefficient (Fig. 5c) is also reduced, showing that the water dipole moments are more correlated as the bilayers come together.

This restriction of water motion by greater proximity to the lipids has been seen both computationally and experimentally. Using simulation, Bhide and Berkowitz (2006) calculated the translational and reorientational rates for the waters in the bulk and in the interfacial and lipid head

group region and found a decrease in their rates as they penetrated into the bilayer. They found that lipid head group motion was a significant factor in this process but did not account for all of the slowdown. Since, on average, the waters will be closer to the lipid head groups as the bilayers come together, there will be reduced motional effects. These effects were measured in an experimental dioleoylphosphatidylcholine (DOPC) system (Ulrich and Watts 1994), where water motion was three times slower at small interbilayer distances vs. full hydration distances. Volke et al. (1994) varied the hydration level from about 30 waters per lipid to 5 waters per lipid and used NMR to calculate the lateral diffusion constant of water for POPC at 296 K, a system very much like ours. Their curve is similar in shape to the one we have calculated and ranges from about 8×10^{-6} cm^2/s when the bilayers are far apart to under 2×10^{-6} cm^2/s when the bilayers are dehydrated to 5 waters per lipid. Our rates are slightly lower, perhaps due to the presence of salt.

This slowdown may only be partially due to hydrogen bonding patterns because recent work (Scodinu and Fourkas 2002) where water was confined in nanopores showed a slowing by a factor of 10 and the authors posited that the slowdown is not due to formation of hydrogen bonds to the lipid head groups but to confinement. Another group (Choudhury and Pettitt 2005) performed simulations bringing two planes of carbon atoms together and found that, similar to our work, there is greater water ordering as the plates approach each other; i.e., both the diffusion constant and the rotational autocorrelation function are decreased.

In order to determine the effect of decreasing bilayer separation on the hydrogen bond network, we calculated hydrogen bonding partners between pairs of water molecules and between a water molecule and the oxygen atoms in the phosphate or glycerol groups of the lipid head group. We found significant changes in the hydrogen bonding characteristics as the bilayer separation decreased. The criterion for a hydrogen bond is a hydrogen-to-acceptor distance of 2.4 Å, which is equivalent to a donor–acceptor distance of about 3.4 Å. An additional angle criterion adds little value because steric clashes between the acceptor and donor enforce this rule automatically (De Loof et al. 1992). As can be seen in Fig. 6a, which shows the average number of hydrogen bonds per water per frame, as the bilayers approach each other, there are fewer waters available for hydrogen bonding, so many instead bond to the phosphates. In Fig. 6b, it is clear that at small interbilayer distances, the hydrogen bond duration for water to phosphate oxygens grows to be quite long, to about 650 ps.

Other computational groups (Bhide and Berkowitz 2005) have also seen that as the water molecules move from the bulk into the interface or are buried in the lipid head groups, they lose some water–water hydrogen bonds but gain hydrogen bonds to the lipids. Essentially, the number of hydrogen bonds per water varied somewhat,

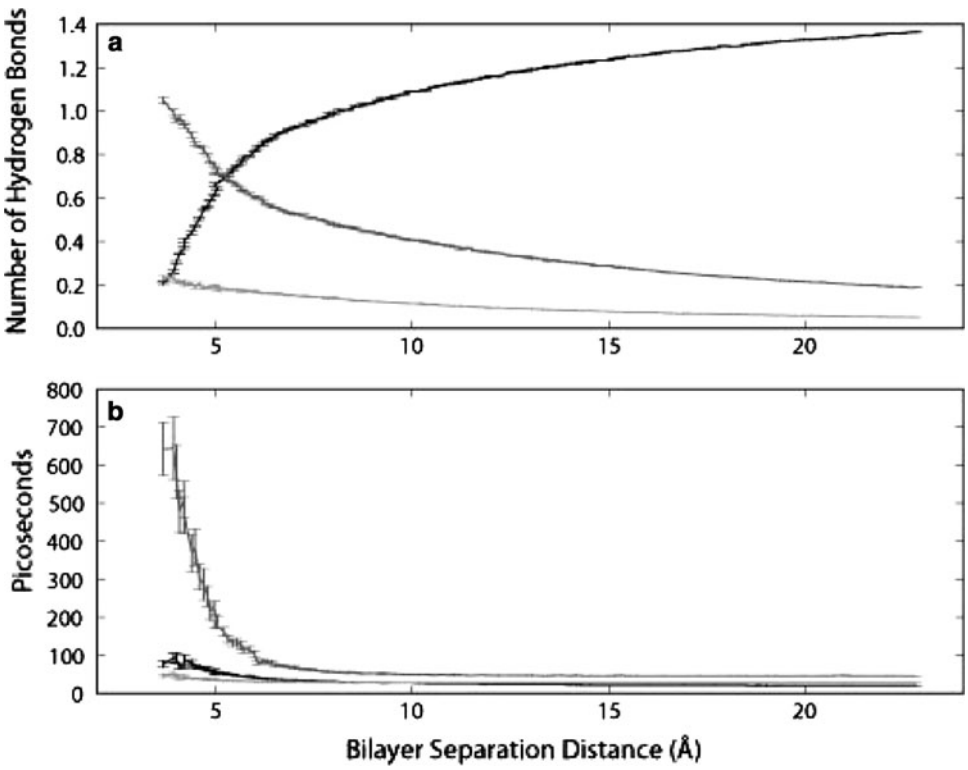

Fig. 6 Hydrogen bonding characteristics between waters (*black*), water hydrogens and lipid phosphate oxygens (*dark gray*) and water hydrogens and lipid glycerol oxygens (*light gray*). **a** The number of hydrogen bonds per frame (normalized by total number of waters available) demonstrates how more hydrogen bonds are made to the phosphate groups as the number of available waters decreases. **b** The average duration of the hydrogen bonds increases at small bilayer separations

though the distribution of hydrogen bonds for each water molecule was more or less unchanged. The variation was due to the different bonding geometries available in the interface and lipid head group regions as well as to an increased strength of hydrogen bonds in those regions. Another group (Pasenkiewicz-Gierula et al. 1997) studied hydrogen bonds in dimyristoylphosphatidylcholine (DMPC) using geometric criteria and found 5.3 bonds to water per lipid, 4.4 with the phosphate oxygens and 0.9 with the glycerol oxygens. Hydrogen bond lifetimes were of the same order of magnitude as what we computed, averaging about 100 ps. They found that 70% of the lipids are linked together by hydrogen-bonded water bridges between lipid neighbors, with average lifetimes of at least 50 ps.

Along with an increase in water order, we also found evidence of greater order in the lipids and salt behavior as the bilayers approach each other. Figures 7 and 8 show how the lipid and salt diffusion rates both slow dramatically as the bilayers come together. Our lipid diffusion rates decrease from 1.2×10^{-8} to 5.4×10^{-10} cm^2/s laterally. The sodium diffusion rate decreases from 2.9×10^{-7} to 1.9×10^{-10} cm^2/s laterally and in the z direction from 1.0×10^{-7} to 3.0×10^{-10} cm^2/s. The chloride diffusion rate decreases from 7.0×10^{-7} to 3.7×10^{-10} cm^2/s laterally and from 6.6×10^{-8} to 6.2×10^{-10} cm^2/s in the z direction. Figure 7b shows the rotational autocorrelation coefficient of the vectors connecting the phosphate group to the choline group of the lipid head groups (PN dipole moment), which is again reduced as the bilayers come to near contact, showing that the dipole moment orientations are more correlated as the bilayers move together.

Experimental evidence confirms the reduction in diffusion rate as bilayers are dehydrated. There is NMR spin-relaxation experimental evidence (Ulrich and Watts 1994) showing a slowing of choline group motion as DOPC bilayers approach each other. Gaede and Gawrisch (2003) measured a reduction in diffusion rates in POPC liposomes from 1.9×10^{-7} cm^2/s in excess water to 8.6×10^{-8} cm^2/s for 8.2 waters/lipid, though in this work the temperature was 322 K. However, definitions for lipid diffusion rates vary, as Sackmann (1995) pointed out when proposing that diffusion had two parts, local motion in its cage and larger diffusional jumps to new sites. Sackmann (1995) used dipalmitoylphosphatidylcholine (DPPC) at 12 wt% water and 60°C and found a lateral diffusion rate of 1×10^{-7} cm^2/s and a local diffusion rate of 2×10^{-7} cm^2/s. The time scales accessible to each experimental technique also vary; macroscopic experiments like fluorescence recovery after photobleaching measure larger millisecond diffusional jumps, yielding values around 4×10^{-8} cm^2/s, while neutron scattering experiments measure local diffusive motion on picosecond timescales and typically see diffusion rates between 1×10^{-7} and 4×10^{-7} cm^2/s (Böckmann et al. 2003). Though millisecond timescales are

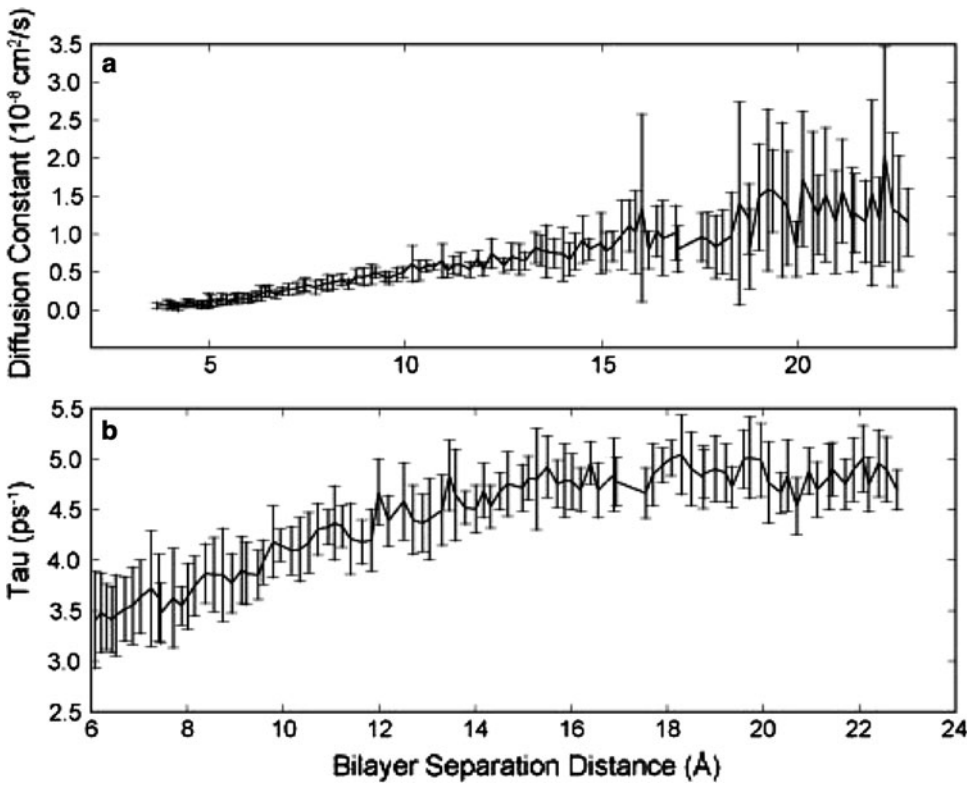

Fig. 7 Lipid diffusion rates and rotational autocorrelation coefficient are both reduced as the bilayers move together: **a** lateral diffusion and **b** coefficient of rotational autocorrelation between dipole moments

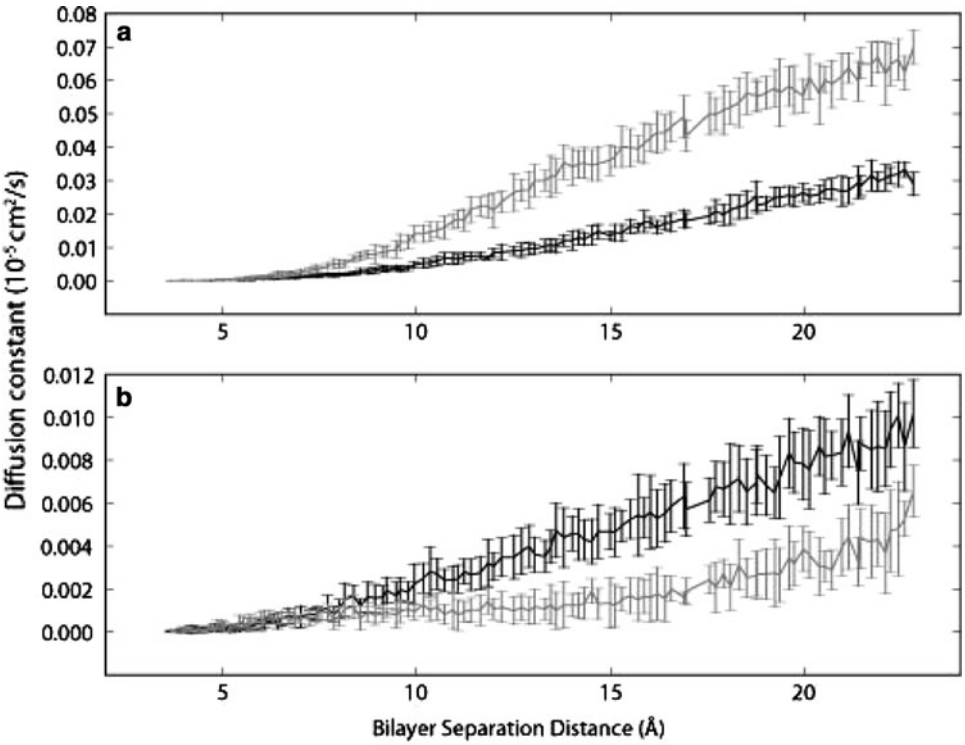

Fig. 8 Ion diffusion rates of chloride (*gray*) and sodium (*black*) slow markedly with bilayer dehydration: **a** lateral diffusion and **b** diffusion in the z direction

inaccessible to atomistic simulations at this point, diffusion rates calculated in simulations correspond to the shorter timescale that can be measured in neutron scattering experiments. Simulation groups (Essmann and Berkowitz 1999) have computed lateral diffusion rates of 3×10^{-7} cm^2/s, which compare well with experimental results. Our rates are lower than these estimates, most likely because they did not include salt in their systems. Böckmann et al. (2003) calculated POPC lipid diffusion constants with NaCl from experiments and simulation. Diffusion rates dropped from 3.9×10^{-8} to 2.6×10^{-8} cm^2/s with the addition of 220 mM salt to their simulated system, so our 1 M salt concentration most likely reduced the diffusion rate significantly. Böckmann et al. (2003) also determined diffusion rates experimentally and found rates of about 2.2×10^{-8} and 1.9×10^{-8} cm^2/s for 1 M NaCl.

These decreases in entropy and increased order are, of course, energetically unfavorable and would lend our free energy curve a repulsive character. However, there may be other enthalpic effects at play that may either compensate for or increase these effects. We calculated the infinite cutoff pairwise enthalpic interaction energies between different groups in the simulations. Considering only the bilayer atoms themselves and ignoring any interactions with the solvent, there is an attractive force from the enthalpic interaction energy between the bilayers, as seen in Fig. 9. Thus, it is clear that the solvent interactions are essential to making the overall relative free energy change repulsive. Similar behavior was observed in work by Pertsin et al. (2007), where there was an attractive character to the direct interaction between the bilayers that was overcome by the repulsive forces due to interactions between the solvent and the bilayers. There are other attractive interactions between two groups, such as phosphate and chloride; but the opposite-sign interaction, of phosphate and sodium in this case, is repulsive. The interactions between the phosphate groups and waters is one example that is not directly compensated for by an opposite-sign attractive interaction (i.e., choline and water) and likely also supplies some repulsive energy. These results, while instructive, are not meant to be taken as quantitative calculations of enthalpy but as a qualitative estimate of the source of enthalpic effects in the system. Likewise, our entropic estimates only include the water, presumably a major source of entropy changes; but nonetheless, it is not possible to expect that summing the entropic and enthalpic estimates made here will yield the free energy change exactly.

At a microscopic level, one would expect to see changes in the lipids that reflect the increasingly strong interactions they are feeling as the bilayers approach. There were no significant changes in lipid chain behavior as measured by lipid S_{CD} order parameter calculations, and the mean tilt angle for the lipid head group PN dipole is also unchanged (data not shown). X-ray diffraction work has shown that the PN dipole is tilted out from the bilayer at full hydration (Kučerka et al. 2006), and in simulation work the angle has been calculated as $73° \pm 0.5°$ (Sachs et al. 2004b) and

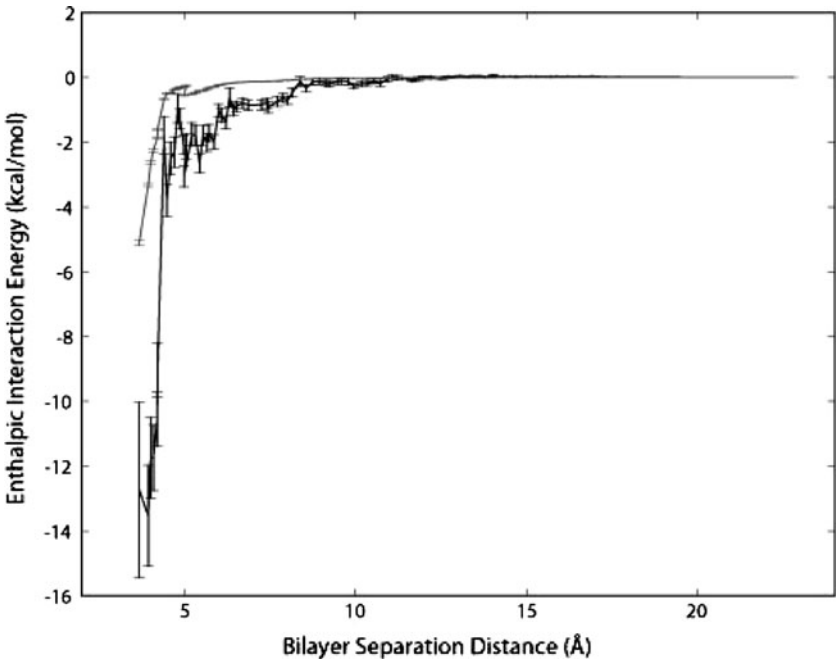

Fig. 9 Infinite cutoff pairwise interaction energy per water between the two bilayers separated into coulombic (*gray*) and van der Waals (*black*) showing an overall attractive interaction

70.6° ± 1.4° (Gurtovenko 2005) from the bilayer normal. Our calculated mean angle values are also in this range. Experimental ^{2}H-NMR studies examining quadrupolar frequency splittings of DOPC (Ulrich and Watts 1994) and POPC (Bechinger and Seelig 1991) show that as the bilayer is dehydrated, the choline group moves toward the tail region. Other simulation work (Mashl et al. 2001) found a similar trend in PN dipole orientation as hydration is varied in DOPC bilayers.

There are also other significant changes in the ordering of water between the bilayers beyond diffusion and reorientational rates. As seen in work of Sachs et al. (2004a) and in Fig. 10, the waters form oriented bands between the two bilayers, with on average more waters closest to the lipid

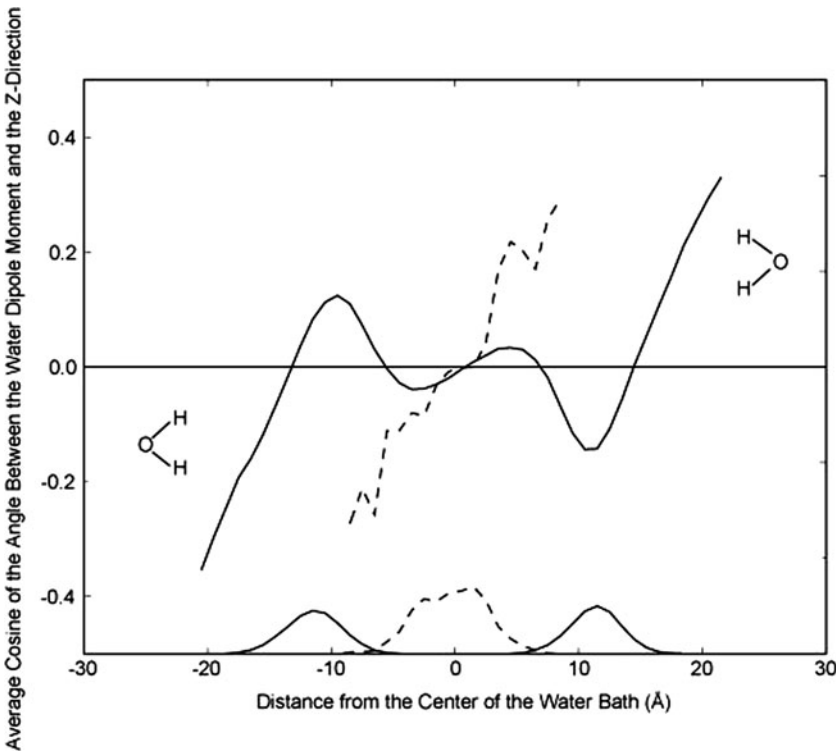

Fig. 10 The cosine of the angle between the water dipole moment and the z direction for the system with 22.79 Å bilayer separation (*solid line*) and 3.94 Å bilayer separation (*dashed*). The peaks below show where the phosphate atoms of the lipid head groups are on average for that system. The bilayer normal direction flips in the center, so the plot is actually symmetric in the z direction. The largest peaks correspond to the oxygen of the water pointing toward the center of the bilayer, and peaks of the opposite sign correspond to the oxygen pointing in the opposite direction

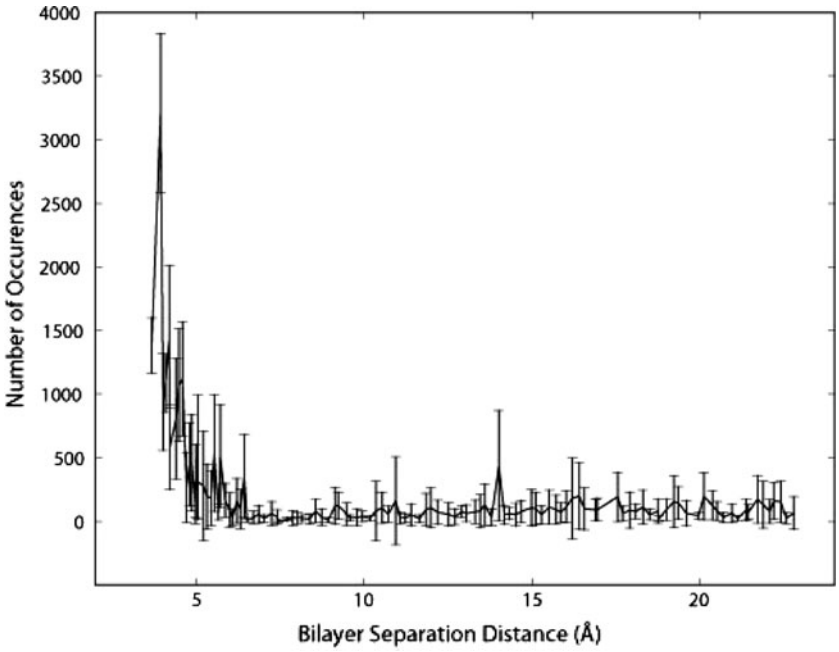

Fig. 11 Propensity for lipid tail groups to splay, a possible antecedent to membrane fusion. The count of how many times the terminal carbons of the lipid tails go into the head group region (cross the average phosphate position over the whole trajectory)

head groups oriented with their oxygen atoms pointed toward the bilayers. Farther out from the lipid head groups, there is a band of water with on average more waters pointed in the opposite direction and a third band the other way. The system is symmetric, so the pattern repeats as we move toward the other monolayer. When the bilayers are much closer together, however, there is most likely not enough room for three distinct bands and there is just one band for each monolayer.

As a final tantalizing thought, we also investigated possible prefusion events as the bilayers approach each other. Previous work (Stevens et al. 2003) has indicated that to begin a fusion event lipids tails may splay, with one tail remaining in its "home" bilayer and one tail reaching into the opposing bilayer. As seen in Fig. 11, we found that many more terminal carbons explored the head group region of their own bilayer as the bilayer got close to each other. Thus, there is a marked increase in possible prefusion splay candidates as the bilayers begin to near one another.

Conclusion

Lipid multilayer systems have been studied experimentally for years using surface force apparatus, atomic force microscopy and osmotic pressure studies; and these studies find strong repulsive forces as the bilayers come together. To reproduce this phenomenon and gain insight into its molecular origins, we performed about 240 all-atom computational molecular dynamics simulations of lipid bilayer systems. We calculated the relative free energy change as the bilayers approach each other and were able to closely reproduce the repulsive behavior seen in experimental systems. We then broke this free energy into entropic and enthalpic components in order to gain greater knowledge of the thermodynamic trends underlying the behavior. The atomistic simulations also capture microscopic adjustments that are seen experimentally as bilayers approach each other: decreases in diffusion constants, slowing of reorientational motion and redistribution of hydrogen bonds as the amount of water decreases.

Acknowledgements We thank Scott Feller for providing our initial POPC structure. We acknowledge support from NIH under R21GM076443 and R01GM064746. Sandia is a multiprogram laboratory operated by Sandia Corporation, a Lockheed Martin Company, for the United States Department of Energy's National Nuclear Security Administration under contract DE-AC04-94AL85000. This work was completed in 2009 as part of the PhD research of Anastasia Gentilcore.

References

Abdulreda MH, Moy VT (2007) Atomic force microscope studies of the fusion of floating lipid bilayers. Biophys J 92:4369–4378

Bechinger B, Seelig J (1991) Conformational changes of the phosphatidylcholine headgroup due to membrane dehydration: a H-2-NMR study. Chem Phys Lipids 58:1–5

Bhide S, Berkowitz M (2005) Structure and dynamics of water at the interface with phospholipid bilayers. J Chem Phys 123:224702

Bhide S, Berkowitz M (2006) The behavior of reorientational correlation functions of water at the water–lipid bilayer interface. J Chem Phys 125:094713

Binder H, Kohlstrunk B, Heerklotz H (1999) Hydration and lyotropic melting of amphiphilic molecules: a thermodynamic study using humidity titration calorimetry. J Colloid Interface Sci 220: 235–249

Böckmann R, Hac A, Heimburg T, Grubmüller H (2003) Effect of sodium chloride on a lipid bilayer. Biophys J 85:1647–1655

Brooks B, Bruccoleri R, Olafson B, States D, Swaminathan S, Karplus M (1983) CHARMM—a program for macromolecular energy, minimization, and dynamics calculations. J Comput Chem 4:187–217

Choudhury N, Pettitt B (2005) Dynamics of water trapped between hydrophobic solutes. J Phys Chem B 109:6422–6429

De Loof H, Nilsson L, Rigler R (1992) Molecular dynamics simulation of galanin in aqueous and nonaqueous solution. J Am Chem Soc 114:4028–4035

Derjaguin BV, Landau L (1941) Theory of stability of highly charged lyophobic sols and adhesion of highly charged particles in solutions of electrolytes. Acta Physicochim URSS 14:633–652

Essmann U, Berkowitz M (1999) Dynamical properties of phospholipid bilayers from computer simulation. Biophys J 76:2081–2089

Feller SE, MacKerell AD (2000) An improved empirical potential energy function for molecular simulations of phospholipids. J Phys Chem B 104:7510–7515

Feller SE, Gawrisch K, MacKerell AD (2002) Polyunsaturated fatty acids in lipid bilayers: intrinsic and environmental contributions to their unique physical properties. J Am Chem Soc 124:318–326

Gaede HC, Gawrisch K (2003) Lateral diffusion rates of lipid, water, and a hydrophobic drug in a multilamellar liposome. Biophys J 85:1734–1740

Gurtovenko A (2005) Asymmetry of lipid bilayers induced by monovalent salt: atomistic molecular dynamics study. J Chem Phys 122:244902

Helfrich W (1978) Steric interaction of fluid membranes in multilayer systems. Z Naturforsch 33:305–315

Hockney R, Eastwood J (1989) Computer simulation using particles. Taylor & Francis, New York

Humphrey W, Dalke A, Schulten K (1996) VMD: visual molecular dynamics. J Mol Graphics 14:33–39

Israelachvili JN (1985) Intermolecular and surface forces. Academic Press, San Diego

Israelachvili JN, Wennerstroem H (1990) Hydration or steric forces between amphiphilic surfaces. Langmuir 6:873–876

Israelachvili JN, Wennerstroem H (1992) Entropic forces between amphiphilic surfaces in liquids. J Phys Chem 96:520–531

Israelachvili JN, Wennerstrom H (1996) Role of hydration and water structure in biological and colloidal interactions. Nature 379:219–225

Jorgensen WL, Chandrasekhar J, Madura JD, Impey RW, Klein ML (1983) Comparison of simple potential functions for simulating liquid water. J Chem Phys 79:926–935

Kučerka N, Tristram-Nagle S, Nagle J (2006) Structure of fully hydrated fluid phase lipid bilayers with monounsaturated chains. J Membr Biol 208:193–202

Lazaridis T (1998) Inhomogeneous fluid approach to solvation thermodynamics. 1. Theory. J Phys Chem B 102:3531–3541

Leikin S, Parsegian VA, Rau DC, Rand RP (1993) Hydration forces. Annu Rev Phys Chem 44:369–395

LeNeveu DM, Rand RP, Parsegian VA, Gingell D (1977) Measurement and modification of forces between lecithin bilayers. Biophys J 18:209–230

Manciu M, Ruckenstein E (2001) Free energy and thermal fluctuations of neutral lipid bilayers. Langmuir 17:2455–2463

Marcelja S, Radic N (1976) Repulsion of interfaces due to boundary water. Chem Phys Lett 42:129–130

Markova N, Sparr E, Wadso L, Wennerstrom H (2000) A calorimetric study of phospholipid hydration. Simultaneous monitoring of enthalpy and free energy. J Phys Chem B 104:8053–8060

Marra J, Israelachvili J (1985) Direct measurements of forces between phosphatidylcholine and phosphatidyethanolamine bilayers in aqueous-electroylyte solutions. Biochemistry 24:4608–4618

Mashl RJ, Scott HL, Subramaniam S, Jakobsson E (2001) Molecular simulation of dioleoylphosphatidylcholine lipid bilayers at differing levels of hydration. Biophys J 81:3005–3015

Mills R (1973) Self-diffusion in normal and heavy-water in range 1–45 degrees. J Phys Chem 77:685–688

Parsegian VA, Fuller N, Rand RP (1979) Measured work of deformation and repulsion of lecithin bilayers. Proc Natl Acad Sci USA 76:2750–2754

Pasenkiewicz-Gierula M, Takaoka Y, Miyagawa H, Kitamura K, Kusumi A (1997) Hydrogen bonding of water to phosphatidylcholine in the membrane as studied by a molecular dynamics simulation: location, geometry, and lipid-lipid bridging via hydrogen-bonded water. J Phys Chem A 101:3677–3691

Pera I, Stark R, Kappl M, Butt HJ, Benfenati F (2004) Using the atomic force microscope to study the interaction between two solid supported lipid bilayers and the influence of synapsin I. Biophys J 87:2446–2455

Pertsin A, Platonov D, Grunze M (2007) Origin of short-range repulsion between hydrated phospholipid bilayers: a computer simulation study. Langmuir 23:1388–1393

Petrache H, Gouliaev N, Tristram-Nagle S, Zhang R, Suter R, Nagle J (1998) Interbilayer interactions from high-resolution X-ray scattering. Phys Rev E 57:7014–7024

Plimpton S (1995) Fast parallel algorithms for short-range molecular dynamics. J Comput Phys 117:1–19

Podgornik R, Parsegian V (1992) Thermal mechanical fluctuations of fluid membranes in confined geometries—the case of soft confinement. Langmuir 8:557–562

Podgornik R, French R, Parsegian V (2006) Nonadditivity in van der Waals interactions within multilayers. J Chem Phys 124:044709

Rand R, Parsegian VA (1989) Hydration forces between phospholipid-bilayers. Biochim Biophys Acta 988:351–376

Ryckaert JP, Ciccotti G, Berendsen HJC (1977) Numerical integration of cartesian equations of motion of a system with constraints molecular dynamics of N-alkanes. J Comput Phys 23:327–341

Sachs J, Crozier PS, Woolf TB (2004a) Atomistic simulations of biologically realistic transmembrane potential gradients. J Chem Phys 121:10847–10851

Sachs J, Nanda H, Petrache H, Woolf T (2004b) Changes in phosphatidylcholine headgroup tilt and water order induced by monovalent salts: molecular dynamics simulations. Biophys J 86:3772–3782

Sackmann E (1995) An empirical potential energy function for phospholipids: criteria for parameter optimization and applications. In: Lipowsky RAS (ed) Handbook of biological physics, vol 1A. Elsevier, Amsterdam, p 213

Schlenkrich MJ, Brickman J, MacKerell AD, Karplus M (1996) Physical basis of self-organization and function of membranes: physics of vesicles. In: Mertz KM, Roux B (eds) Biological membranes: a molecular perspective from computation and experiment. Birkhäuser, Boston, p 31

Scodinu A, Fourkas JT (2002) Comparison of the orientational dynamics of water confined in hydrophobic and hydrophilic nanopores. J Phys Chem B 106:10292–10295

Sornette D, Ostrowsky N (1986) Importance of membrane fluidity on bilayer interactions. J Chem Phys 84:4062–4067

Stevens MJ, Hoh J, Woolf T (2003) Insights into the molecular mechanism of membrane fusion from simulation: evidence for the association of splayed tails. Phys Rev Lett 91:188102

Ulrich AS, Watts A (1994) Molecular response of the lipid headgroup to bilayer hydration monitored by H-2-NMR. Biophys J 66:1441–1449

Verwey EJW, Overbeek JTG (1948) Theory of the stability of lyophobic colloids. Elsevier, New York

Volke F, Eisenblatter S, Galle J, Klose G (1994) Dynamic properties of water at phosphatidylcholine lipid–bilayer surfaces as seen by deuterium and pulsed field gradient proton NMR. Chem Phys Lipids 70:121–131

Zwanzig RW (1954) High-temperature equation of state by a perturbation method 1. Nonpolar gases. J Chem Phys 22:1420–1426